

ON-LINE APPENDIX

TFCE Method

TFCE is an imaging-based voxel-clustering technique that takes into account the neighborhood information of voxels; it provides better sensitivity and more interpretable output than traditional voxel-based methods.¹ An ROI imaging volume of tumor location is composed of a 3D grid of voxels, and each voxel may be assigned a binary value denoting either tumor or normal brain.

Survival Cutoff Robustness Analysis

Previously, different thresholds (top and bottom 25% of data, ≤ 1.5 and > 3 years, and so forth) were set to define poor and good survival groups.^{2–5} Our training dataset was stratified into 3 survival groups on the basis of 3 months below and above the median of overall survival observed in patients with GBM (~ 14 months), respectively. The middle group of patients was excluded in the subsequent survival analysis to ensure a clear distinction between good and poor survival. Our survival histogram exhibits a left skewed distribution in which most patients have poor survival (Fig 1B). To our knowledge, this is the first study systematically evaluating the dependence of finding a significant association between tumor location and having either poor or good survival on the choice of criteria for inclusion in either group. We explored 286 pairs of lower and upper cutoffs in the overall survival at 3–15 months and 15–36 months to determine good and poor survival groups, respectively. Each combination of survival pairs was used to define a poor survival group and a good survival group and was run for the prognostic region sensitivity analysis. Of the 286 survival pairs examined, 120 did not generate results. As a strong indication of the robustness of the results, the voxels generated from the 166 different survival pairs all fell in the same region when superimposed on one another (On-line Fig 1), despite the number of voxels varying depending on the cutoff pair used (On-line Fig 2). The number of voxels that differs substantially among the different survival pairs may be an issue of feature selection to select the optimal number of voxels to avoid underfitting or overfitting.

This analysis included the survival pair previously used by Ellingson et al (12 and 36 months).⁶ No voxels were found to be significantly (P value $< .05$) associated with poor survival (On-line Fig 2), possibly due to the small size in the good survival group ($n = 8$). When the lower and upper cutoffs were 12 and 34 months, voxels were found to be in the right periventricular temporal and occipital white matter (On-line Figs 1 and 2), consistent with the findings of Ellingson et al.⁶

Anatomic Structural Labels from the Talairach Atlas

The Talairach atlas provides 3D anatomic labels of brain locations in the Montreal Neurological Institute coordinate space.⁷ We superimposed each patient's imaging volume on the Talairach atlas to extract the anatomic labels for the voxels significantly associated with survival.

Molecular and Genetic Analysis

The enrichment of the hypoxia/HIF1A pathway in group I was further validated by using genes in the "HIF signaling pathway" in the KEGG to compute single-sample GSEA scores, as previously described.⁸ The significance level for single-sample GSEA scores between the 2 location groups was evaluated by using a boxplot and Student *t* test.

Discrete copy number alterations (amplified or deleted), obtained from the cBioPortal for Cancer Genomics of Memorial Sloan Kettering Cancer Center (<http://www.cbiportal.org/public-portal/index.do>),⁹ were used to validate results.

REFERENCES

- Smith SM, Nichols TE. Threshold-free cluster enhancement: addressing problems of smoothing, threshold dependence and localization in cluster inference. *Neuroimage* 2009;44:83–98 CrossRef Medline
- Patel VN, Gokulrangan G, Chowdhury SA, et al. Network signatures of survival in glioblastoma multiforme. *PLoS Comput Biol* 2013;9: e1003237 CrossRef Medline
- Smoll NR, Schaller K, Gautschi OP. Long-term survival of patients with glioblastoma multiforme (GBM). *J Clin Neurosci* 2013;20: 670–75 CrossRef Medline
- Burton EC, Lamborn KR, Forsyth P, et al. Aberrant p53, mdm2, and proliferation differ in glioblastomas from long-term compared with typical survivors. *Clin Cancer Res* 2002;8:180–87 Medline
- Krex D, Klink B, Hartmann C, et al; German Glioma Network. Long-term survival with glioblastoma multiforme. *Brain* 2007;130(pt 10): 2596–606 CrossRef Medline
- Ellingson BM, Lai A, Harris RJ, et al. Probabilistic radiographic atlas of glioblastoma phenotypes. *AJNR Am J Neuroradiol* 2013;34: 533–40 CrossRef Medline
- Lancaster JL, Woldorff MG, Parsons LM, et al. Automated Talairach atlas labels for functional brain mapping. *Hum Brain Mapp* 2000; 10:120–31 Medline
- Verhaak RG, Hoadley KA, Purdom E, et al; Cancer Genome Atlas Research Network. Integrated genomic analysis identifies clinically relevant subtypes of glioblastoma characterized by abnormalities in PDGFRA, IDH1, EGFR, and NF1. *Cancer Cell* 2010;17:98–110 CrossRef Medline
- Gao J, Aksoy BA, Dogrusoz U, et al. Integrative analysis of complex cancer genomics and clinical profiles by using the cBioPortal. *Sci Signal* 2013;6:pl1 CrossRef Medline
- Méndez-Gómez HR, Vicario-Abejón C. The homeobox gene Gsx2 regulates the self-renewal and differentiation of neural stem cells and the cell fate of postnatal progenitors. *PLoS One* 2012;7:e29799 CrossRef Medline
- Jörnsten R, Abenius T, Kling T, et al. Network modeling of the transcriptional effects of copy number aberrations in glioblastoma. *Mol Syst Biol* 2011;7:486 CrossRef Medline
- Puputti M, Tynninen O, Sihto H, et al. Amplification of KIT, PDGFRA, VEGFR2, and EGFR in gliomas. *Mol Cancer Res* 2006;4: 927–34 CrossRef Medline
- Jackson EL, Garcia-Verdugo JM, Gil-Perotin S, et al. PDGFR alpha-positive B cells are neural stem cells in the adult SVZ that form glioma-like growths in response to increased PDGF signaling. *Neuron* 2006;51:187–99 CrossRef Medline

On-line Table 1: Talairach anatomic structural labels of the prognostic voxels^a

Talairach ID	Cerebrum	Lobe	Gyrus	Tissue and Cell Type	% Voxels Significantly Associated with Survival
52	Right	Temporal	Subgyral	White matter	41.1
174	Right	Sublobar	Lateral ventricle	CSF	30.7
348	Right	Sublobar	Extranuclear	White matter	11.3
664	Right	Limbic	Posterior cingulate	White matter	10.5
320	Right	Occipital	Subgyral	White matter	4.7

^a The Talairach brain atlas was used to extract the anatomic labels of the voxels associated with poor survival with false discovery rate < 0.05 in the training Stanford University Medical Center cohort.

On-line Table 2: GSEA analysis showing statistically significant gene enrichment difference between groups I and II with a family-wise error rate < 0.05^a

	Name	Size	ES	NES	NOM P Value	FDR Q Value	FWER P Value	Rank at Max
Top gene sets that were enriched in Group I (FWER P < .05) ^a								
1	MENSE_HYPoxIA_UP ^a	70	0.67870116	2.8425374	0	0	0	1050
2	ELVIDGE_HIFIA_TARGETS_DN ^{a,b}	83	0.651353	2.785036	0	0	0	1303
3	ELVIDGE_HIFIA_AND_HIF2A_TARGETS_DN ^a	93	0.63277183	2.744839	0	0	0	1303
4	REACTOME_3_UTR_MEDiated_TRANSLATIONAL_REGULATION	88	0.62074935	2.7073562	0	0	0	3248
5	KEGG_RIBOSOME	71	0.6138948	2.6045315	0	0	0	2885
6	BILANGES_SERUM_AND_RAPAMYCIN_SENSITIVE_GENES	60	0.6385915	2.5883207	0	0	0	2885
7	WINTER_HYPoxIA_UP ^a	67	0.6173566	2.570896	0	0	0	2627
8	REACTOME_PEPTIDE_CHAIN_ELONGATION	70	0.6216674	2.5650892	0	0	0	2885
9	REACTOME_TRANSLATION	125	0.5528574	2.5588062	0	0	0	2790
10	REACTOME_INFLUENZA_VIRAL_RNA_TRANSCRIPTION_AND_REPLICATION	84	0.5916988	2.5493844	0	0	0	3047
11	ELVIDGE_HYPoxIA_BY_DMOG_UP ^a	119	0.5507677	2.544955	0	0	0	971
12	REACTOME_ACTIVATION_OF_THE_MRNA_UPON_BINDING_OF_THE_CAP_BINDING_COMPLEX_AND_EIFS_AND_SUBSEQUENT_BINDING_TO_43S	50	0.62746	2.4630954	0	0	0	3148
13	ELVIDGE_HYPoxIA_UP ^a	154	0.5155066	2.461791	0	0	0	1607
14	REACTOME_INFLUENZA_LIFE_CYCLE	115	0.5471523	2.4547613	0	0	0	3248
15	REACTOME_METABOLISM_OF_PROTEINS	329	0.46597627	2.4373863	0	0	0	3248
16	REACTOME_FORMATION_OF_THE_TERNARY_COMPLEX_AND_SUBSEQUENTLY_THE_43S_COMPLEX	42	0.6474824	2.4199326	0	0	0	3148
17	BILANGES_SERUM_RESPONSE_TRANSLATION	31	0.68680006	2.4155636	0	0	0	2790
18	REACTOME_SRp_DEPENDENT_COTRANSLATIONAL_PROTEIN_TARGETING_TO_MEMBRANE	91	0.5440073	2.383955	0	4.98E-05	.001	2885
19	REACTOME_NONSENSE_MEDIATED_DECAY_ENHANCED_BY_THE_EXON_JUNCTION_COMPLEX	89	0.5430242	2.376912	0	4.72E-05	.001	2885
20	FARDIN_HYPoxIA_UP ^a	25	0.7119723	2.372483	0	4.49E-05	.001	740
21	KIM_WTI_TARGETS_UP	190	0.4736407	2.3274534	0	8.44E-05	.002	2806
22	MEISSNER_BRAIN_HCP_WITH_H3K27ME3	174	0.4702482	2.288893	0	2.00E-04	.005	2568
23	KIM_HYPoxIA ^a	24	0.68347996	2.266775	0	2.30E-04	.006	1294
24	SCHUHMACHER_MYC_TARGETS_UP	73	0.5405023	2.2483792	0	2.20E-04	.006	2566
25	KOBAYASHI_EGR_SIGNALING_6HR_DN	18	0.7315822	2.2417624	0	2.12E-04	.006	1657
26	CHNG_MULTIPLE_MYELOMA_HYPERPOloid_UP	45	0.588231	2.240852	0	2.03E-04	.006	3205
27	LEONARD_HYPoxIA ^a	41	0.60017943	2.2281919	0	2.28E-04	.007	2449
28	CROMER_METASTASIS_DN	71	0.5179916	2.2045023	0	3.13E-04	.01	1851
29	KARLSSON_TGFBI_TARGETS_UP	100	0.49586993	2.1855402	0	5.13E-04	.016	2278
30	BILD_HRAS_ONCOGENIC_SIGNATURE	194	0.44362888	2.1791706	0	5.26E-04	.017	2012
31	LUI_THYROID_CANCER_CLUSTER_3	24	0.6698309	2.1781957	0	5.09E-04	.017	2636
32	SCHLOSSER_MYC_TARGETS_AND_SERUM_RESPONSE_UP	42	0.5792902	2.1762977	0	5.47E-04	.019	2387
33	SEMENZA_HIFI_TARGETS ^a	34	0.6079476	2.1643827	0	7.69E-04	.028	2323
34	FLOTTO_PEDIATRIC_ALL_THERAPY_RESPONSE_UP	47	0.5590184	2.155238	0	8.77E-04	.033	2841
35	QI_HYPoxIA_TARGETS_OF_HIFI_A_AND_FOXA2 ^a	31	0.617345	2.1522675	0	8.52E-04	.033	2846
36	AMIT_EGF_RESPONSE_480_HELA	144	0.4580991	2.1485944	0	8.77E-04	.035	1814
37	YAO_TEMPORAL_RESPONSE_TO_PROGESTERONE_CLUSTER_14	113	0.4659112	2.126359	0	0.0012	.047	2330

Continued on next page

On-line Table 2: Continued

	Name	Size	ES	NES	NOM P Value	FDR Q Value	FWER P Value	Rank at Max
Top gene sets that were enriched in Group II (FWER, $P < .05$) included interferon signatures								
1	BROWNE_INTERFERON_RESPONSE_GENES	62	-0.76571715	-3.1721227	0	0	0	2226
2	WIELAND_UP_BY_HBV_INFECTON	92	-0.7035768	-3.155526	0	0	0	2077
3	SANA_RESPONSE_TO_IFNG_UP	52	-0.771993	-3.1099284	0	0	0	1754
4	DAUER_STAT3_TARGETS_DN	45	-0.77884096	-3.0551095	0	0	0	1036
5	WALLACE_PROSTATE_CANCER_RACE_UP	251	-0.57892776	-3.0158305	0	0	0	2051
6	REACTOME_INTERFERON_ALPHA_BETA_SIGNALING	53	-0.7300165	-2.9478784	0	0	0	1447
7	HECKER_IFNB1_TARGETS	72	-0.6780474	-2.9288445	0	0	0	1415
8	MOSERLE_IFNA_RESPONSE	24	-0.8550822	-2.886646	0	0	0	1036
9	EINAV_INTERFERON_SIGNATURE_IN_CANCER	25	-0.80567455	-2.756376	0	0	0	740
10	BOSCO_INTERFERON_INDUCED_ANTIVIRAL_MODULE	57	-0.6602913	-2.725239	0	0	0	2196
11	WINTER_HYPOXIA_DN	37	-0.72811	-2.6942258	0	0	0	916
12	RADAЕVA_RESPONSE_TO_IFNA1_UP	51	-0.68123895	-2.6706812	0	0	0	1447
13	FULCHER_INFLAMMATORY_RESPONSE_LECTIN_VS_LPS_DN	326	-0.49438652	-2.6614952	0	0	0	2883
14	REACTOME_INTERFERON_GAMMA_SIGNALING	47	-0.67947733	-2.6371546	0	0	0	1492
15	KIM_LRRRC3B_TARGETS	28	-0.7571561	-2.618386	0	0	0	1017
16	BOWIE_RESPONSE_TO_TAMOXIFEN	77	-0.8585343	-2.617779	0	0	0	882
17	ICHIBA_GRAFT_VERSUS_HOST_DISEASE_D7_UP	85	-0.58986926	-2.5895762	0	0	0	2016
18	REACTOME_INTERFERON_SIGNALING	129	-0.5468976	-2.5823088	0	0	0	1492
19	FARMER_BREAST_CANCER_CLUSTER_1	35	-0.7103986	-2.5749073	0	0	0	1051
20	FLECHNER_BIOPSY_KIDNEY_TRANSPLANT_REJECTED_VS_OK_UP	79	-0.58496696	-2.560673	0	0	0	2103
21	STAMBOLSKY_TARGETS_OF_MUTATED_TP53_DN	37	-0.6806421	-2.543687	0	0	0	2085
22	BENNETT_SYSTEMIC_LUPUS_ERYTHEMATOSUS	27	-0.7421388	-2.542955	0	0	0	1570
23	DER_IFN_ALPHA_RESPONSE_UP	70	-0.5882885	-2.5200293	0	0	0	2016
24	KRASNOSELSKAYA_IF3_TARGETS_UP	37	-0.66648686	-2.4731889	0	0	0	1296
25	ZHANG_INTERFERON_RESPONSE	23	-0.771846	-2.4724002	0	0	0	2196
26	SMID_BREAST_CANCER_NORMAL_LIKE_UP	420	-0.44619134	-2.470256	0	0	0	2406
27	BOWIE_RESPONSE_TO_EXTRACELLULAR_MATRIX	16	-0.81629765	-2.4645834	0	0	0	1172
28	UROSEVIC_RESPONSE_TO_IMIQUIMOD	21	-0.77233535	-2.4492524	0	0	0	882
29	NIELSEN_SYNOVIAL_SARCOMA_DN	18	-0.7868145	-2.4454043	0	0	0	2032
30	TAKEDA_TARGETS_OF_NUP98_HOXA9_FUSION_3D_UP	133	-0.50649303	-2.4396377	0	0	0	2033
31	SEITZ_NEOPLASTIC_TRANSFORMATION_BY_8P_DELETION_UP	66	-0.57668406	-2.4241884	0	0	0	695
32	KEGG_GRAFT_VERSUS_HOST_DISEASE	29	-0.67479974	-2.396564	0	3.52E-05	.001	631
33	KEGG_AUTOIMMUNE_THYROID_DISEASE	38	-0.6357137	-2.3848622	0	3.41E-05	.001	1415
34	KEGG_ALLOGRAFT_REJECTION	30	-0.6733114	-2.380505	0	3.31E-05	.001	1492
35	LEE_DIFFERENTIATING_T_LYMPHOCYTE	135	-0.5043278	-2.3788574	0	3.22E-05	.001	2361
36	WANG_RESPONSE_TO_GSK3_INHIBITOR_SB216763_UP	226	-0.45795664	-2.3626423	0	3.13E-05	.001	2317
37	RODRIGUES_THYROID_CARCINOMA_ANAPLASTIC_DN	353	-0.42716336	-2.3173652	0	1.23E-04	.004	3274
38	REACTOME_CYTOKINE_SIGNALING_IN_IMMUNE_SYSTEM	227	-0.44584024	-2.3160698	0	1.20E-04	.004	2114
39	GRAESSMANN_RESPONSE_TO_MC_AND_SERUM_DEPRIVATION_UP	151	-0.46732438	-2.3154469	0	1.16E-04	.004	1857
40	MORI_MATURE_B_LYMPHOCYTE_UP	70	-0.53322744	-2.3103313	0	1.14E-04	.004	2350
41	DER_IFN_BETA_RESPONSE_UP	96	-0.5080434	-2.2973738	0	1.39E-04	.005	2033
42	BOYAULT_LIVER_CANCER_SUBCLASS_G3_DN	47	-0.5825193	-2.289848	0	1.63E-04	.006	2114
43	ZHU_CMV_8_HR_UP	43	-0.58585054	-2.2857454	0	1.59E-04	.006	1357

Continued on next page

On-line Table 2: Continued

	Name	Size	ES	NES	NOM P Value	FDR Q Value	FWER P Value	Rank at Max
44	KEGG_ANTIGEN_PROCESSING_AND_PRESENTATION	63	-0.5513464	-2.285256	0	1.55E-04	.006	1044
45	PICCALLUGA_ANGIOMUNOBLASTIC_LYMPHOMA_UP	170	-0.4631262	-2.284144	0	1.52E-04	.006	3040
46	BOQUEST_STEM_CELL_DN	187	-0.45363614	-2.2792203	0	1.49E-04	.006	2284
47	MCLACHLAN_DENTAL_CARIES_UP	220	-0.44185755	-2.2647667	0	1.45E-04	.006	2699
48	WILENSKY_RESPONSE_TO_DARAPLADIB	27	-0.6485103	-2.2610154	0	1.66E-04	.007	2395
49	KEGG_TYPE_I_DIABETES_MELLITUS	36	-0.6109174	-2.2552688	0	1.63E-04	.007	631
50	TAKEDA_TARGETS_OF_NUP98_HOXA9_FUSION_10D_UP	138	-0.47754347	-2.2512286	0	1.60E-04	.007	1386
51	MCLACHLAN_DENTAL_CARIES_DN	216	-0.4347533	-2.235594	0	2.69E-04	.012	2699
52	GAURNIER_PSMD4_TARGETS	61	-0.5413288	-2.233296	0	2.64E-04	.012	829
53	SCHUETZ_BREAST_CANCER_DUCTAL_INVASIVE_UP	321	-0.41682082	-2.2281508	0	2.80E-04	.013	2699
54	ICHIBA_GRAFT_VERSUS_HOST_DISEASE_35D_UP	105	-0.48243406	-2.2265925	0	3.38E-04	.016	1364
55	ZHAN_MULTIPLE_MYELOMA_PR_DN	32	-0.6058919	-2.2253203	0	3.31E-04	.016	1210
56	RUIZ_TNC_TARGETS_UP	138	-0.45652333	-2.2206259	0	3.46E-04	.017	3510
57	SANA_TNF_SIGNALLING_UP	73	-0.5247185	-2.2164314	0	4.01E-04	.02	2362
58	TAKEDA_TARGETS_OF_NUP98_HOXA9_FUSION_8D_UP	116	-0.4731359	-2.2112947	0	4.34E-04	.022	1484
59	MORI_LARGE_PRE_BI_LYMPHOCYTE_DN	48	-0.55875385	-2.2080102	0	4.65E-04	.024	2189
60	ZHAN_MULTIPLE_MYELOMA_LB_DN	33	-0.61817664	-2.2050157	0	4.95E-04	.026	2098
61	RODWELL_AGING_KIDNEY_UP	343	-0.40871465	-2.188697	0	6.37E-04	.034	1654
62	RICKMAN_TUMOR_DIFFERENTIATED_WELL_VS_MODERATELY_UP	67	-0.5133985	-2.17391	0	7.57E-04	.041	3481

Note: FWER indicates family-wise error rate; FDR = false discovery rate; ES, enrichment score; NES, normalized enrichment score; NOM, nominal; Max, maximum.

^a Hypoxia- and HIF-1-related pathways. Three of the top 6 gene sets enriched in group I were hypoxia and HIF-1-related pathways.

^b ELVIDGE_HIF1A_TARGETS_DN pathway contains genes downregulated after knockdown of HIF1A.

On-line Table 3: Molecular subtype distributions for groups I and II in the TCGA dataset^a

	Proneural	Neural	Classic	Mesenchymal	Total
Group I, overlapping	7	3	4	6	20
Group II, nonoverlapping	26 (including 4 G-CIMP)	20	26	31	103
Total	33	23	30	37	123

Note:—G-CIMP indicates glioma-CpG island methylator phenotype.

^a Group I overlapping with prognostic regions; group II, nonoverlapping with prognostic regions.

On-line Table 4: Gene annotation of amplified genes in group I compared with group II^a

Gene ID	Gene Name	FDR Q Value	Chromosome Location	GO Functional Enrichment/Literature Citations
GSX2	GS homeobox 2	0	4q12	Forebrain dorsal/ventral pattern formation; neuron fate specification ¹⁰
CHIC2	Cysteine-rich hydrophobic domain 2	0	4q12	CHIC2 and PDGFR regulate GBM stem cell markers and other neural differentiation markers ¹¹
RPL21P44	Ribosomal protein L21 pseudogene 44	0	4q12	—
KIT	Mast/stem cell growth factor receptor Kit	0	4q12	PDGFRA and KIT are commonly amplified in GBM ¹²
PDGFRA	Platelet-derived growth factor receptor, alpha polypeptide	0	4q12	PDGFRA is marker for neural stem cells in the adult SVZ that form gliomalike growths in response to increased PDGF signaling ¹³

Note:—GO indicates gene ontology; ID, identifier; FDR, false discovery rate.

^a Copy number analysis of log2 copy number data showed genes amplified in group I (tumor involving the prognostic right peritumoral location) and their GO annotations.

On-line Table 5: Contingency table showing a significant association between PDGFRA amplification and the grouping by the prognostic location in the TCGA cohort^a

	PDGFRA Amplification	PDGFRA Normal Level	Total
Group I, overlapping	6	15	21
Group II, nonoverlapping	10	100	110
Total	16	115	131

^a Analyzing discrete copy number alteration data showed that amplifications of PDGFRA (Fisher exact test, 2-tailed $P = .023$) were significantly associated with group I.

On-line Table 6: Contingency table showing a significant association between CHIC amplification and the grouping by the prognostic location in the TCGA cohort^a

	CHIC Amplification	CHIC Normal Level	Total
Group I, overlapping	6	15	21
Group II, nonoverlapping	9	101	110
Total	15	116	131

^a Analyzing discrete copy number alteration data showed that amplifications of CHIC (Fisher exact test, $P = .016$) were significantly associated with group I.

On-line Table 7: Contingency table showing a significant association between GSX2 amplification and the grouping by the prognostic location in the TCGA cohort^a

	GSX2 Amplification	GSX2 Normal Level	Total
Group I, overlapping	6	15	21
Group II, nonoverlapping	10	100	110
Total	16	115	131

^a Analyzing discrete copy number alteration data showed that amplifications of GSX2 (Fisher exact test, $P = .023$) were significantly associated with group I.

On-line Table 8: Contingency table showing a significant association between KIT amplification and the grouping by the prognostic location in the TCGA cohort^a

	KIT Amplification	KIT Normal Level	Total
Group I, overlapping	5	16	21
Group II, nonoverlapping	7	103	110
Total	12	119	131

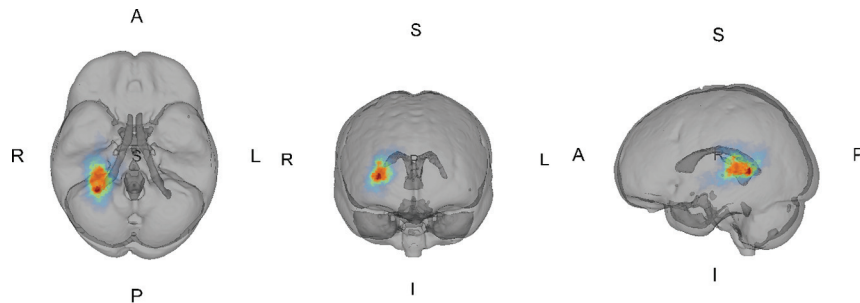
^a Analyzing discrete copy number alteration data showed that amplifications of KIT (Fisher exact test, $P = .025$) were significantly associated with group I.

On-line Table 9: PDGFRA amplification maintains the significant association with the right periatrional location in intermediate-sized tumors and in the restricted subset of intermediate and large tumors

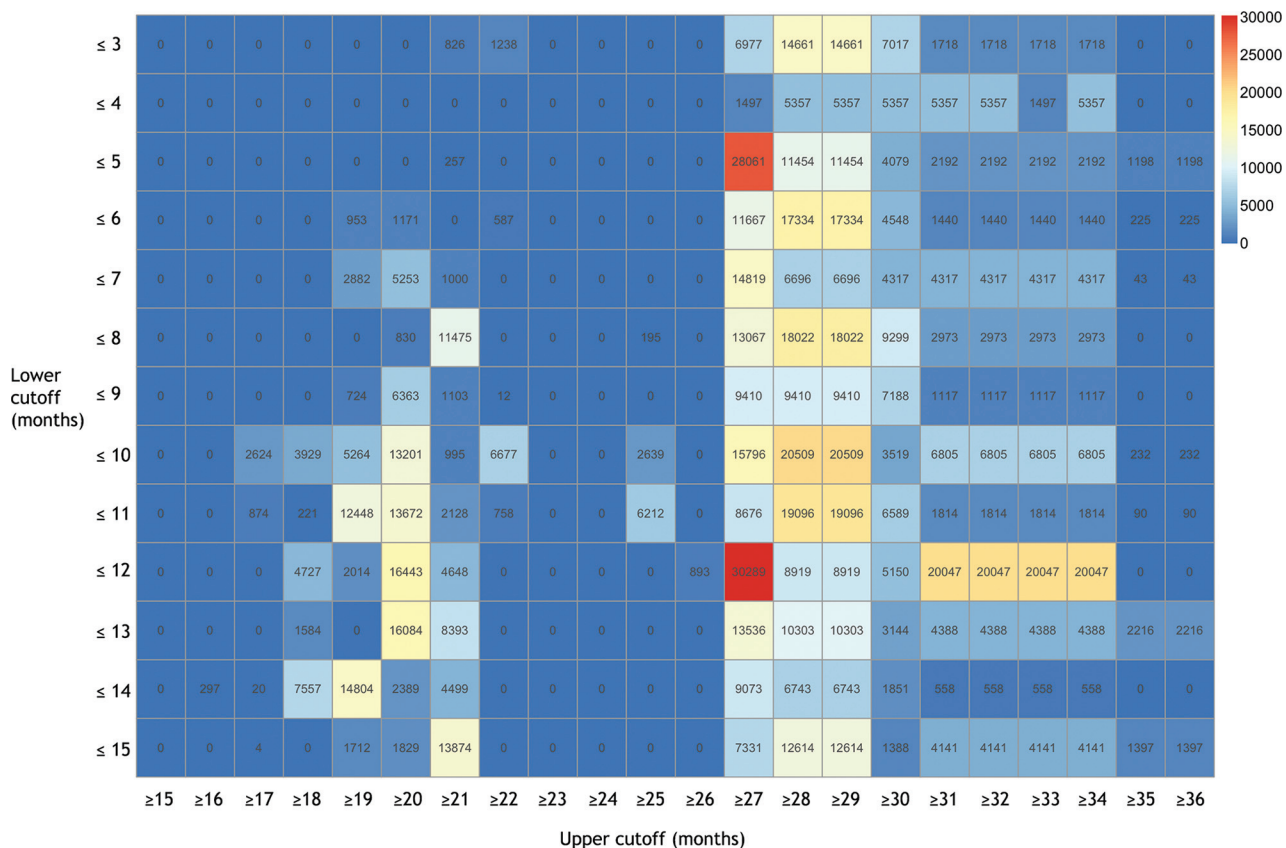
	PDGFRA Amplification	PDGFRA Normal Copy Number	Total
Intermediate tumors ^a			
Group I, overlapping	4	6	10
Group II, nonoverlapping	3	40	43
Total	7	46	53
Intermediate and large tumors ^b			
Group I, overlapping	6	13	19
Group II, nonoverlapping	8	66	74
Total	14	79	93

^a N = 53; Fisher exact test, 2-tailed P = .018.

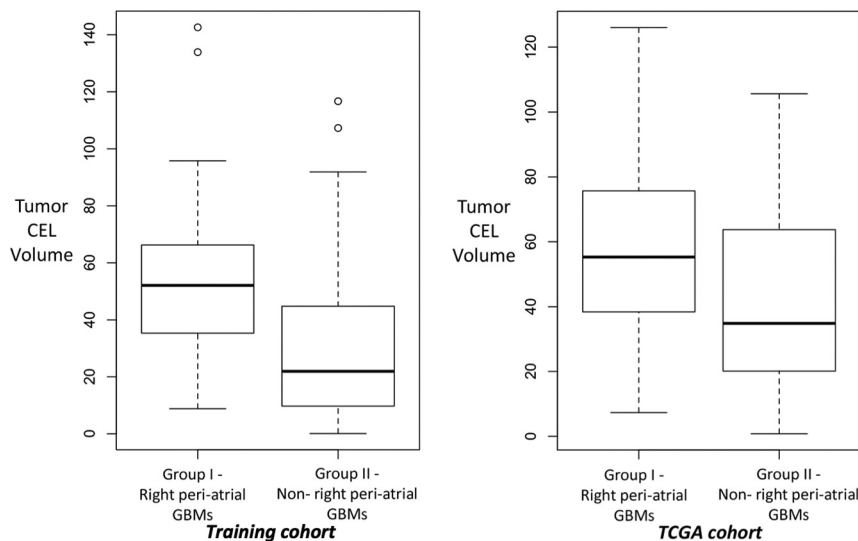
^b N = 93; Fisher exact test, 2-tailed P = .035.



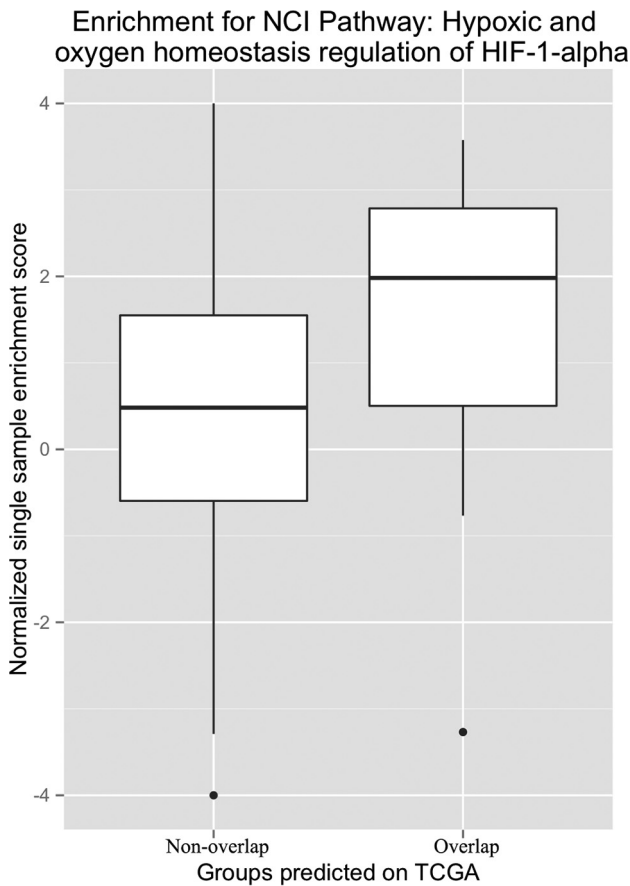
ON-LINE FIG 1. Survival robust analysis by different pairs of survival. The axial, coronal, and sagittal views of the 3D frequency map of voxels generated by different survival cutoff pairs (P value < .05). The voxels associated with poor survival by different pairs of survival all fell into the same periventricular white matter region adjacent to the posterior lateral ventricle of the SVZ, indicating the robustness of the analysis.



ON-LINE FIG 2. Evaluation of the number of significant voxels (false discovery rate < 0.05) for each cutoff pair. The x-axis indicates the upper cutoffs from >15 to 15 months; the y-axis, lower cutoff from >15 to 36 months. The intersection of each row and column is color-coded to indicate the number of significant voxels for the pair of cutoffs evaluated.



ON-LINE FIG 3. Boxplots of GBM CEL volume for the 2 groups (group I: right peri-atrial GBMs; group II, non-right peri-atrial GBMs) in the training (left) and the test (right) cohorts, respectively. The mean of CEL volume of group I GBMs is 1.8 times the size of group II ($n = 40$ versus 206, $P < 1.5e-6$) in the Stanford University Medical Center cohort and 1.4 times in the TCGA cohort ($n = 21$ versus 110, $P < .01$).



ON-LINE FIG 4. Boxplots for single-sample GSEA scores for the 2 groups. Single-sample GSEA scores between the 2 groups for NCI pathway “hypoxic and oxygen homeostasis regulation of HIF-1- α ” suggest that the hypoxia pathway was enriched in group I (Wilcoxon P value = .0072) compared with group II.